Effective trapping of cold atoms using dipole and radiative forces in an optical trap

Taro Mashimo,[*] Masashi Abe, and Satoshi Tojo

Department of Physics, Chuo University, Kasuga, Bunkyo-ku, Tokyo 112-8551, Japan

We report on the stable effective trapping of cold rubidium atoms by a method for a single optical trap in the near-optical resonant regime. An optical trap with the near-optical resonance condition consists of not only the dipole but also the radiative forces, while a trap using a far-off resonance dominates only the dipole force. We measure the spatial behaviors of the center-of-mass positions and the loading efficiencies of the trapped atoms in the near-optical resonant trap, by changing the detuning over the range of -0.373 to -2.23 THz from the D_2 resonance. The time dependence of the spatial behavior in the trap indicates that the suitable positions for stably holding atoms are altered because the equilibrium condition between the optical dipole and the radiative forces depends on the trap laser detuning. The stable position, which is not a primary position of focus in the Gaussian beam optics, depends only on the laser detuning due to the change in the radiative force, while it is independent of the change in the laser intensity, which results in a balance between the radiative and dipole forces.

I. INTRODUCTION

Optical control of particles and materials is one of the powerful techniques for investigating phenomena of the media for precise observations under the condition of highly qualified isolations [1]. After the experimental realization of the optical control of cold atoms by the optical tweezer [2], this optical technique is applied to broad research fields such as those involving gaseous atoms [3,4], dielectric and metal particles [5,6], and viruses and bacteria [7]. Moreover, the optomechanical techniques have been used for realizing precise allocation of atoms [8], levitation of nanoparticles to investigate isolated thermal phenomena [9], etc. In general, the optomechanics applications have been realized by the dipole forces only since the radiative force is not dominant in a far-off resonant regime. However, there do exist some radiative effects in far-off resonant regimes [10].

For fundamental research studies, the optical forces have been developed in the research field of cold atoms because sufficient low-density conditions in typical cold atom experiments allow atomic collisions to be studied under the two-body problem so the cold atom experiments are in excellent agreement with theoretical predictions. A far-off resonant trap (FORT), which has large detuning from the resonance with more than several tens of THz typically [10], can hold cold atoms and quantum degenerates in any spin states for investigating collision properties [11] and spinor Bose–Einstein condensates without heating and dephasing the quantum states [12], and to change the shapes of the trap potential and spatial controls of the atoms [13,14]. The applications of the research in the FORT mainly involve the use of the dipole forces, called an optical *dipole force* trap. Moreover, a near-optical resonant trap (NORT), which has a small detuning round of several tens of GHz to several THz, has been treated with experimentally

harsh conditions because of the scattering effects beyond their perturbative conditions by the spontaneous emission [15–17]. The scattering effect generated by the radiative force induces dephasing of quantum states, degradation of observation precision, and heating due to spontaneous emission with absorption [18]. In Ref. [17], the properties of trapped particles near the focus position of the trap laser beam with near-optical regimes have been investigated under the condition of oil as the surrounding medium and nano ruby-spheres as the particles' trapped nano ruby-spheres immersed in a medium with similar real refractive index to the typical oil immersion lenses. They estimated the trapping efficiencies of the nano ruby-spheres with a high numerical aperture beam. There is a possibility of using not only the dipole force but also the radiative force as the hybrid force trap for an observation of a time evolution during no heating, no scattering, and no dephasing.

The NORT has significant properties owing to its near-resonant regime. In view of spin states of atoms, one can change magnitudes of electric dipole moments of spin states coupled with the NORT laser and generate differences of the effective trap potential depths between different spin states by tuning optical polarization from linear to circular polarizations [19]. In the case of the linear polarization of the NORT laser, the transition strengths of spin states are equivalent. On the other hand, in the case of the circular and elliptical polarizations, the transition strengths of spin states are different. In any polarizations of the FORT laser far from D_1 and D_2 resonances, the transition strengths of spin states are identical due to averaging out of the strengths between D_1 and D_2 transitions.

In this study, we demonstrate the NORT properties with single cold rubidium atoms; similar research performed by Ref. [17] studied nano ruby-spheres which are much larger than gaseous rubidium atoms. We have investigated the hybrid potential comprising the dipole and the radiative forces in the NORT regime in the range of sub-THz to several THz

*taro.mashimo@gmail.com

detunings from the resonance. We have also evaluated the equilibrium trap conditions including the dipole and radiative effects and found that the equilibrium positions from our experimental results are in good agreement with the calculations under the condition of a stable hybrid potential in a single optical trap.

II. THEORY

A. Dipole and radiative force potentials in the NORT

The trap beam potential using laser light typically can be described by the theory of Gaussian beam optics [20]. The electric field amplitude of the propagating beam along the z axis near the Rayleigh region is approximated as

$$E(r, z) = \frac{E_0}{\sqrt{1 + (z/z_0)^2}} \exp\left[-\frac{r^2}{w^2(z)}\right], \qquad (1)$$

where $w(z) = w_0\sqrt{1 + (z/z_0)^2}$ is the radius of the beam, w_0 is the beam waist, $z_0 = k w_0^2/2$ is the confocal parameter, and E_0 is the amplitude of the electric field at the center of the beam waist of the trap laser beam. The interaction between the atom and the trap laser beam produces the dipole and the radiative forces in the atomic cloud in the trap region [21]. If the detuning of the laser from the atomic resonance δ is sufficiently larger than the natural width of the resonance Γ and the saturation parameter $s = (\mu^2 E^2/2\hbar^2)/(\delta^2 + \Gamma^2/4) \ll 1$, where μ is the electric dipole moment of an atom, the potentials induced by the optical dipole and the radiative forces at the beam axis U_D and U_R are approximated as

$$U_D = -\frac{\mu^2}{4\hbar} \frac{E_0^2}{\delta} \frac{z_0^2}{z^2 + z_0^2}, \qquad (2)$$

$$U_R = \frac{\mu^2}{4\hbar} \frac{k_z \Gamma}{2\pi} \frac{E_0^2 z_0}{\delta^2} \tan^{-1}\left(\frac{z}{z_0}\right), \qquad (3)$$

where k_z is a z component of the wave vector. In the case of the FORT, the radiative force is negligible due to $|\delta| \gg (k_z z_0 \Gamma)/(4\pi)$ [15]. Therefore, the trap is called an optical *dipole* trap. However, in the case of the NORT, there is a possibility of the existence of an equilibrium condition with variables δ and z due to the presence of the radiative force. As a result, the dipole and radiative forces generate a hybrid trap potential and change the position of the potential local maximum. The change in the position due to the hybrid trap forces from that in the optical dipole force is defined as an equilibrium position. The equilibrium position, or the displacement from the initial position, z_{eq} is caused by the condition, which is the local minimum value of $U_D + U_R$ [Eqs. (2) and (3)], and is expressed as the solution of the equation $z^2 - (4\pi z|\delta|)/(k_z \Gamma) + z_0^2 = 0$ with $-z_0 < z < z_0$ as

$$z_{eq} = \frac{2\pi |\delta|}{k_z \Gamma} - \sqrt{\left(\frac{2\pi |\delta|}{k_z \Gamma}\right)^2 - z_0^2}. \qquad (4)$$

Equation (4) indicates that $|\delta| > (k_z^2 w_0^2 \Gamma)/(8\pi^2)$ in the presence of equilibrium. Figure 1 illustrates a typical geometry that the cold atoms in the NORT exhibit. Owing to the radiative force potential, the total potential of the trap is modified as the hybrid potential from the dipole and the radiative force potentials. The change of the equilibrium position, indicated
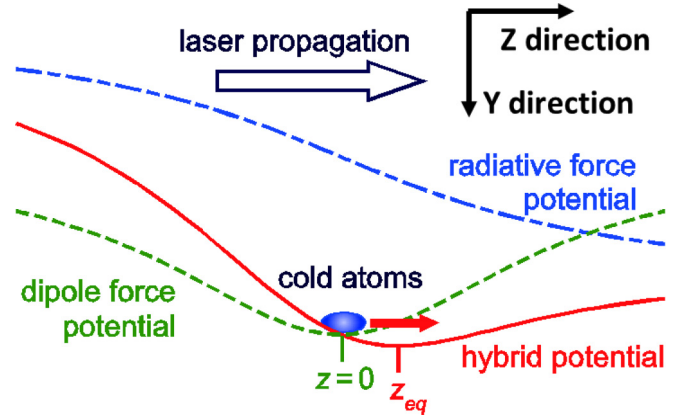
FIG. 1. Geometry of the cold atoms in the NORT. The trapped atoms located in the focal point experience imbalanced effects of the dipole and the radiative forces generating the hybrid potential along with the beam axis of the trap laser.

as z_{eq}, generates variable oscillating motions of the trapped atoms from the initial position $z = 0$. We note that the equilibrium position is independent of the electric field amplitude E_0 as shown in Eq. (2).

B. Loading efficiency at a finite temperature in the NORT

The loading rate of a typical magneto-optical trap (MOT) to an optical trap depends on the profile of the trap beam, including the effect of gravity and the temperature of the cold atomic cloud [22]. The axially symmetric potential generated by the dipole force potential mainly determines the loading rate, and the additional potential generated by the radiative force affects atoms along the beam axis. Owing to the depth of the dipole force potential, the loaded atoms can be trapped on the axis despite the existence of the radiative force potential. The optical dipole force potential in the case of $s \ll 1$ can be expressed as

$$U_D \simeq \frac{\hbar \Gamma^2}{8\delta} \frac{I}{I_s}, \qquad (5)$$

where I is the laser intensity, and $I_s = 2\pi hc\gamma/(3\lambda^3)$ is the saturation intensity. The trap generated by a typical laser beam has a two-dimensional Gaussian profile on the cross section perpendicular to the beam axis. By using the electric field of the trap as expressed in Eq. (1), the trap potential in Eq. (5) can be rewritten as

$$U_D(r, z) = \frac{\epsilon_0 \hbar \Gamma^2}{16 I_s \delta} \frac{w_0^2 E_0^2}{w^2(z)} \exp\left[-\frac{2r^2}{w^2(z)}\right]. \qquad (6)$$

By considering the gravity effect, the net trap potential should be modified as $U_D' = U_D(r, z) - mgy$, where the y axis is along the direction of the gravitational force with $y = 0$ at the center of the trap beam. In the condition of the horizontal trap with a typical confinement of the laser system for ultracold atoms, the gravitational potential term mgy can be approximated to be constant [23].

A cold atomic cloud is typically loaded into the optical trap up to an energy of $1/10$ of the potential depth [22,23]. We regard this energy as the threshold limit, below which

the optical trap can hold lower-velocity atoms in accordance with the Maxwell–Boltzmann distribution at a finite temperature. The trapped number of atoms in unit length at the z axis is expressed as the cumulative distribution function of the Maxwell–Boltzmann distribution $h_{\mathrm{MB}}(T, U(r))$ from the atoms with the velocity below the threshold limit in the potential $U(r)$ at a temperature of T. By using modified trap potential with the effect of gravity, we can derive the total number of trapped atoms expressed as

$$N = n_0 \int_{-z_a}^{z_a} \int_0^{r_a} h_{\mathrm{MB}}(T, U_{\mathrm{D}}'(r)) 2\pi r\, dr\, dz, \qquad (7)$$

where n_0 is atomic cloud density at the temperature T and r_a is the radius of the atomic cloud.

III. EXPERIMENTAL SETUP

A. Cooling and NORT sequence

The experimental apparatus and procedure used for ultracold ^{87}Rb atoms are almost the same as those described in Ref. [23], except for the optical trap system. We prepare cold ^{87}Rb atoms in a vacuum chamber using a conventional MOT scheme. The cooling beam is detuned at -20 MHz from the $5\,^2S_{1/2}$ $F = 2$ to $5\,^2P_{3/2}$ $F' = 3$ transition, and the repump beam is resonant to the $F = 1$ to $F' = 2$ transition. After precooling the Rb atoms, we turn off the magnetic-field gradient after the compression of the MOT and start the polarization gradient cooling (PGC), which consists of two parts. In the first part, the detuning of the cooling laser is swept from -32 to -80 MHz with a 25% decrease of the initial intensity. The second part starts with a frequency jump of the laser locking point from the $F' = 3$ peak to the $F' = 2, 3$ crossover peak. This jump shift corresponds to -133 MHz detuning. We use a commercially available laser servo controller (Vescent Photonics Inc., D2-125), which enables the frequency jump with a sample-and-hold circuit. The repump beam detuning is set to -123 MHz to obtain gray-molasses cooling [24,25]. After the second part, 1.8×10^8 atoms at less than $5\,\mu$K are typically produced with the cancellation of the residual magnetic field using three Helmholtz coil pairs for highly effective PGC. We estimate the residual field to be less than 50 mG. Then the optical trap beam is switched on after the atom cloud of diameter approximately $400\,\mu$m is cooled with the cooling and repump beams. The optical trap beam is irradiated into the molasses for 65 ms to load atoms into the optical trap. After the loading to the trap, the atoms which are out of the trap fall off and are separated from the atoms in the trap. The loading of atoms is completed in this period. The cooling and repumping beams are turned off. We hold atoms in the trap by altering the holding time to as much as 200 ms. At the end of holding time, the atoms are irradiated by a weak repumping beam and excited to the $F' = 2$, following which almost all the atoms are pumped to the $F = 2$ state. The number of atoms and temperature of the atoms in the optical trap are measured through absorption imaging after the time of flight.
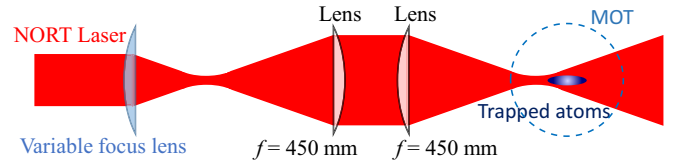
FIG. 2. Experimental geometry of the NORT. By changing in the focal length of the variable focus lens, the beam parameters of the NORT can be controlled.

B. The NORT apparatus

Figure 2 shows the experimental geometry of our NORT. The trap beam is generated from a semiconductor laser and the detuning is adjusted from the D$_2$ line from -0.37 to -2.23 THz. The beam passes through a single-mode optical fiber to clean up its spatial mode and to improve the spatial stability of the laser beam. The collimated trap laser beam also passes through the expanding lens system, which consists of a variable focus lens with a clear aperture of 2.5 mm and a fixed focus lens with $f = 450$ mm for the tight focusing condition, and is focused on the atomic cloud by a lens with $f = 450$ mm. The focal length of the variable lens is set at approximately 75 mm to achieve the focus condition at the center of the molasses cloud. The beam profile can be approximated to be a circle and the focal point can be displaced by changing the focal length of the variable focus lens in the range of $f = 60 - 91$ mm. The beam optical power is set from 7.8 to 62.4 mW with linear polarization along the horizontal axis. The range of the potential depths is estimated to be from $k_{\mathrm{B}} \times 20$ to $k_{\mathrm{B}} \times 300\,\mu$K. The volumes and depths of the trap are dominant for the loading efficiency from the ultracold atomic clouds in the optical molasses condition [23]. By using a tilted 785-nm band-pass filter, we suppress the other longitudinal modes which are outside of the target frequency, to reduce the scattering and heating effects in the NORT.

IV. RESULTS AND DISCUSSION

We measure the remaining number of atoms in the NORT with a holding time of 20 ms after loading under change in the focal length of the variable focus lens in the range of $60 - 91$ mm with $\delta = -1.256$ THz for the detuning of the trap laser. We also tune the NORT laser power at 15.6, 31.2, 46.8, and 62.4 mW, as shown in Fig. 3(a). Each point represents an average value over three samples, with the standard deviation as the error bar. The temperatures of atoms in the NORT are approximately $10\,\mu$K. The dependence of the number of trapped atoms on the focal length of the variable focus lens shows symmetricity centered around the focal point in the trap laser beam. When the laser power is high, there are two peaks for the number of trapped atoms, whereas only a single peak is observed for low power values of the laser.

We have numerically calculated the number of trapped atoms using the cumulative distribution function of the Maxwell–Boltzmann distribution for a temperature of $10\,\mu$K for the atomic clouds, as expressed in Eq. (7). Figure 3(b) shows the calculation results with one fitting parameter normalized to compensate for the average number of atoms in
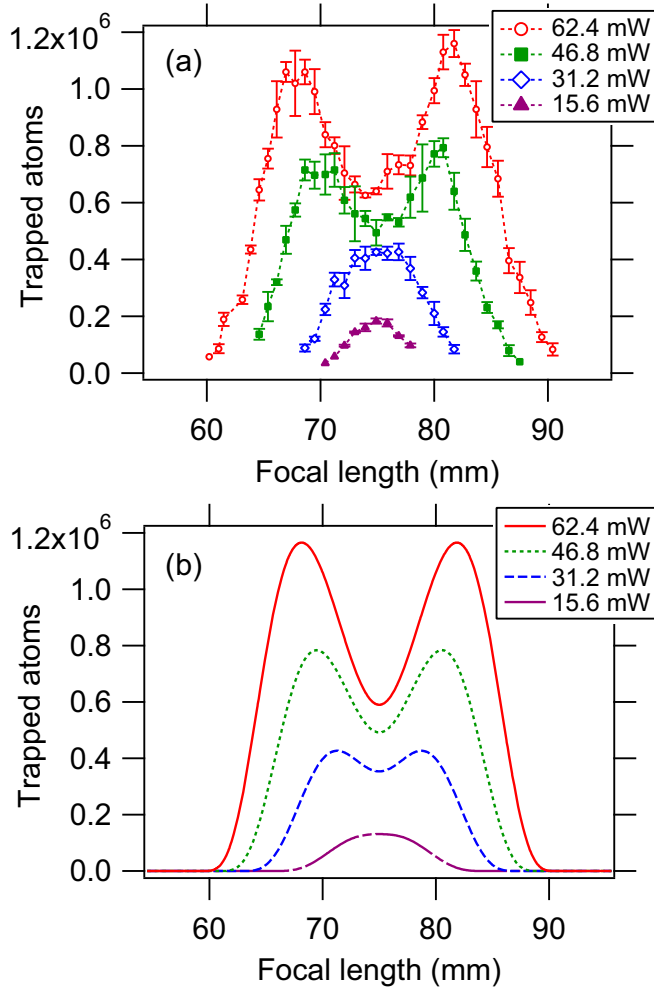
FIG. 3. Focal length dependence of the number of atoms: (a) Experimental results at 62.4 mW (open circles), 46.8 mW (closed squares), 31.2 mW (open diamonds), and 15.6 mW (closed triangles). (b) Calculations with a single experimental parameter of the number of atoms at 62.4 mW (solid line), 46.8 mW (dotted line), 31.2 mW (dashed line), and 15.6 mW (dotted-dashed line).

FIG. 4. Trap time dependence of the center-of-mass positions of the trapped atoms in the NORT. The focal lengths of the variable focus lens are 75.98 (closed triangles), 75.50 (closed circles), 75.02 (closed squares), 74.54 (open circles), 74.06 (open triangles), and 73.58 mm (open squares). The lines are the fitting curves of the oscillation function obtained from Eq. (8).

the two peaks in the experiment with 62.4 mW of the NORT intensity. As we considered in Sec. II B, the trap efficiency is affected, and the number of atoms is reduced by gravity, especially at the branch side of the optical trap. The effect of gravity corresponding to 1 μK generates the shallow potential to reduce the trapped atoms. With respect to the potential of the NORT, the radiative force generates the additional potential along the beam axis, whereas the dipole force constructs the axially symmetric potential, gathering cold atoms in the initial holding positions. Owing to the characteristics of the additional potential in the NORT, the potential depth in the radial direction remains unchanged, whereas that in the axial direction is modified. The displacement of the atomic cloud is insensitive to the efficiency of atom trapping in the NORT. The calculation results are in good agreement with those of the experiments, especially when the two peaks can be explained as large trapping volumes that are dominant in the higher power regime. In our experimental condition of the temperature of the atomic cloud, the effective net trapping

volumes of both branch sides are larger than that of the focus region. In the case of low power, the calculation results are comparable to those of the experiments for the number of atoms in the trap, although there are some differences for the dependence on focal length. The potential depth of the trap in the low power regime is sensitive to the beam profile of the trap, such as the spatial mode and tilted angle from the horizontal plane of the beam, which reduces the total trap depth generated by the dipole force. In addition, the effective net trapping volumes of both branch sides are smaller than that of the focus region. The agreement between the calculations and experimental results indicates that the dipole force of the NORT mainly determines the efficiency of initial atom loading, whereas the radiative force has no effect on the initial loading rate.

Then we have measured the time evolution of the trapped atomic cloud in the NORT. The trapped atoms start to move in the trap along the general axial direction. Because the hybrid trap of the NORT produces an additional radiative force on the atoms as compared to the FORT beam. Figure 4 illustrates the time evolution of the center-of-mass positions of atomic clouds in the NORT for different focal lengths. Here, the focal lengths of the variable focus lens are 75.98, 75.50, 75.02, 74.54, 74.06, and 73.58 mm, with a detuning of -1.256 THz and trap laser power of 31.2 mW. We define the evolution time $t = 0$ ms as just time after finishing the loading into the NORT with the gray molasses. The initial positions of the atoms are located at the center of the molasses. The zero point of the relative center-of-mass position is defined as the initial position for the focal length of 75.02 mm at $t = 0$ ms. The relative center-of-mass positions of the atomic clouds have displacements with oscillationlike behaviors. When the focal length is larger than 75 mm, the atomic cloud moves to the beam propagating direction, which is the positive in Fig. 4. On the other hand, when the length is less than 75 mm, the atoms move to negative side. We confirm that there exist the
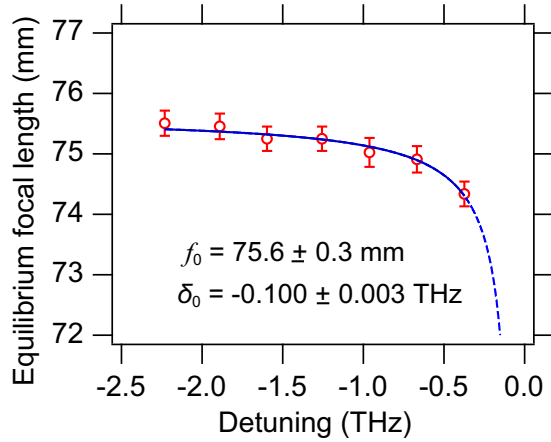
FIG. 5. Detuning dependence of the equilibrium focal length in balance. The solid curve is fitted to the right of Eq. (4). The dashed line is the extrapolated estimation using the fitting parameters. The fitting results show that the equilibrium focal length $f_0 = 75.6 \pm 0.3$ mm and the threshold of detuning $\delta_0 = -0.100 \pm 0.003$ THz for trapping capability.

limitations to the amplitude for both the positive and negative regions. The limitation for positive region is caused by the focus position that is across the atomic position. When the focus position is closer to the initial atomic center position, the direction of the radiation and the dipole forces are on the same side from the focus, then the atoms in the NORT move out of the trap. The limitation for the negative region is from the limitation of dipole force to capture atoms in the trap. Owing to the additional potential of the NORT, the radiative force deforms the trap potential along the beam axis. In the region of the Rayleigh length, the behaviors of atoms initially located at defocused points can be regarded as a cosine function. Therefore, in Fig. 4, we fit the experimental data with the function

$$z(t) = A\cos(\omega t + \theta) + z_1, \qquad (8)$$

where ω is the angular frequency of the oscillation, z_1 is the offset value of the oscillation, and A is the oscillation amplitude of the atomic cloud in the NORT. We consider that the trapped atoms at the initial positions with approximately zero velocity start oscillating in the NORT harmonically with the oscillator potential at $\theta = \pi$.

We have determined the dependence of the amplitudes A from Fig. 4 on each focal length. By linearly fitting the amplitudes A depending on the focal length f, we can find the equilibrium focal length at the zero-crossing point as $A = 0$ and then estimate $f = 75.08$ mm for $\delta = -1.256$ THz. In the case of $A = 0$, the atomic cloud tends to stay at the initial position because the dipole and the radiative forces of the NORT are canceled at equilibrium condition. The equilibrium focal length is regarded as the most stable position to hold the atoms for a longer trap time. It should be noted that we have fitted the amplitude in the range of more than a few millimeters away from the focus in the initial position and confirmed larger amplitudes with nonharmonic oscillations rather than cosine oscillations. Figure 5 shows the equilibrium focal length for each frequency of detuning derived from
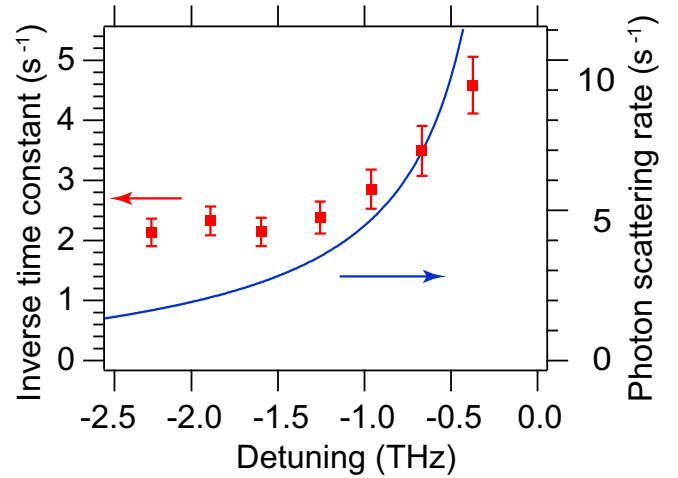
FIG. 6. Detuning dependence of inversed lifetimes of trapped atoms in equilibrium conditions. The solid line denotes the photon scattering rates of the NORT on the beam axis.

estimation of the nonoscillation focal length with $A = 0$ for each trap time dependence of the center-of-mass positions as those in Fig. 4. For the comparison of the same trap depth, the laser power values of the NORT are set to 7.8, 17.5, 25.3, 32.5, 43.4, 52.2, and 65.1 mW, corresponding to the frequency detunings $\delta = -0.373, -0.668, -0.962, -1.256, -1.598, -1.891,$ and -2.232 THz, respectively. The equilibrium focal lengths near resonance under $\delta > -1.0$ THz suddenly decrease with decreasing the absolute detuning $|\delta|$, whereas those under $\delta < -1.0$ THz decrease only slightly. We fit the detuning dependence of the equilibrium focal length using Eq. (4) with $z_{eq} = f_0 - f$, where f_0 is the asymptote focal length. The fitting results can be in a suitable range of the experimental results, and the asymptote having the value of $f_0 = 75.6 \pm 0.3$ mm is close to the focus of the trap beam in the far-off resonant regime. We have confirmed that there is no equilibrium condition in threshold conditions close to the resonance of $\delta \sim -0.15$ THz in our experiments and the results are comparable to the fitting values of the divergence condition in the detuning case of $\delta_0 = -0.100 \pm 0.003$ THz. The threshold for the divergence is determined by the confocal parameter z_0 and the detuning δ, as expressed by Eq. (4), and it is insensitive to the laser power. So a threshold detuning to enable to trap atoms is $\delta = (k_z^2 w_0^2 \Gamma)/(8\pi^2)$.

The radiative force in small δ can generate not only an additional force of the optical trap but also the undesired heating effect caused by the photon scattering. Figure 6 shows the detuning dependence of the inverse time constants of the trapped atoms with the equilibrium focal conditions, and that of the photon scattering rate of the NORT. The experimental results are fitted by the single exponential function, owing to one body loss of the trapped atoms in our experimental condition [23]. In the condition of $\delta > -1.0$ THz, the inverse time constant increases, owing to the large effect of the radiative force, as shown in Fig. 6. The detuning dependence of the inverse time constants is similar to that of the photon scattering rates. Nevertheless, the quantitative differences in the inverse of time constant in $\delta > -1.0$ THz are only a few factors larger in magnitude than those in $\delta < -1.0$ THz. The

results indicate that the NORT in the hybrid trap condition near detuning from sub- to several THz can be applied to ultracold experiments.

The equilibrium displacement z_{eq} depends on both the inverse of the trap laser detuning and the confocal parameter as shown in Eq. (4). We normalize the z_{eq} and derive the value of R as a normalization constant. The ratio of the equilibrium displacement to the confocal parameter, defined as $R = z_{eq}/z_0$, informs us of the experimental conditions for realization of the hybrid trap system. In our NORT system, we can estimate the experimental value of $R = 0.030$ with $z_{eq} = 94$ μm at $\delta = -2.23$ THz, and $R = 0.40$ with $z_{eq} = 1.26$ mm at $\delta = -0.373$ THz. The results are comparable to the calculation results: $R = 0.068$ with $z_{eq} = 215$ μm at $\delta = -2.23$ THz and $R = 0.51$ with $z_{eq} = 1.61$ mm at $\delta = -0.373$ THz, respectively. The values of R at the NORT are one or two orders of magnitude larger than those in the FORT for the same optical conditions; e.g., in the system using $\lambda = 1064$ nm, $R = 0.0015$ generates $z_{eq} = 6.33$ μm at $\delta = -102$ THz in our trap system. It is roughly estimated that the threshold for the realization of the hybrid trap regime is $R = 0.01$ for the condition where the range of the Rayleigh length in a single trap is a few millimeters. The NORT system has large advantages in comparison with the FORT system because in large detuning the value R is approximately proportional to $1/|\delta|$ and is independent of the laser power. The sensitivity to the confocal parameter indicates that the radiative force can help the off-resonant trap with additional degrees of freedom as the spatial mode, such as the Laguerre–Gaussian mode [26,27]. In addition, the trap system used in the typical FORT with large R can be realized with a large value of the confocal parameter; e.g., $R = 0.1$ generates $z_{eq} = 40.1$ mm with $z_0 = 339$ mm in $\delta = -102$ THz with $f = 500$ mm and 1 mm of the beam radius. Regardless of the traps with large $|\delta|$ such as the general optical tweezer generated by FORT, the hybrid trap can be applied for precise optical control of not only gaseous atoms but also nanoscopic and mesoscopic media, owing to the effect of the remaining radiative force on the optical-trap potential.

As an additional advantage, the NORT requires a much lower trap laser intensity to create the effective potential depth on atoms compared to the FORT. It can be applied to the optical implements which can be used only under the condition of weak laser intensity such as variable focus lens in our experiment.

There is another aspect of the NORT method that we can control, namely the transition strength of atoms, depending on their spin states. We can also change the effective trap potential of atoms. For the quantum gas in an optical lattice, phase transition between the superfluid to the Mott insulator has been investigated [28]. The transition between two states depends on the potential depth of optical lattice expressed as the recoil energy of atoms in the lattice, $E_r = \hbar^2 k^2/(2m)$. By doubling the recoil energy from $7E_r$ to $16E_r$, we can control the transition between the Mott insulator to the superfluid phases clearly.

By using the trap laser in the near-optical resonant regime, we can generate the different potential depths for corresponding to the spin states. When the NORT laser has a frequency close the to Rb D_2 line, the transition strengths of the NORT are defined as P_{mF}. The ratio of the potential depth of spin states at ground state $F = 1$ in the NORT near D_2 resonance is $P_{-1} : P_0 : P_1 = 5 : 4 : 3$. Whereas the NORT laser frequency is close to D_1 line, the ratio at $F = 1$ are $P_{-1} : P_0 : P_1 = 1 : 2 : 3$ while the ratio in the FORT is $1 : 1 : 1$. One can have phase control of the atom and also control the transition between the Mott insulator and superfluid phases.

V. CONCLUSION

We have established a method of hybrid optical trapping, which comprises both the dipole and the radiative forces using the laser light in the near optical resonant regime, and we name the trap the NORT. We have measured the number of trapped atoms depending on the focal length of the variable focal lens and the oscillation behaviors in the NORT depending on the detuning of the trap laser from the atomic resonance. We have calculated the number of atoms using the Gaussian beams with the cumulative function of the Maxwell-Boltzmann distribution at finite temperature. The calculated results are in good agreement with the experimental results and express the larger number of atoms located at defocused positions. We have estimated the equilibrium position in the case of the NORT and confirmed its power-independent position by comparisons between the experiments and calculations. The trap potential is modified to the displacements along the beam propagation axis, and the displacements are insensitive to the trap laser beam power. The optical tweezer system, including the radiative force, can be applied to precisely control nano- and micro-particles and mesoscopic media during use of multiple traps and higher spatial mode of the trap beams.

Owing to the NORT method, it is expected that one can control the effective trap potential depth of trapped atoms for their own spin states. From this property, it will be possible to generate different atomic phases at the same position in the NORT. For example, one can create two quantum phases, which are the superfluid and the Mott insulator phases [28] at the same position in NORT. The NORT method can open a window to study the combination of these two states because of being able to generate them at the same position.

[1] D. G. Grier, Nature **424**, 810 (2003).

[2] S. Chu, J. E. Bjorkholm, A. Ashkin, and A. Cable, Phys. Rev. Lett. **57**, 314 (1986).

[3] J. D. Miller, R. A. Cline, and D. J. Heinzen, Phys. Rev. A **47**, R4567 (1993).

[4] T. L. Gustavson, A. P. Chikkatur, A. E. Leanhardt, A. Görlitz, S. Gupta, D. E. Pritchard, and W. Ketterle, Phys. Rev. Lett. **88**, 020401 (2001).

[5] A. Ashkin, J. M. Dziedzic, J. E. Bjorkholm, and S. Chu, Opt. Lett. **11**, 288 (1986).

[6] K. Svobada and S. M. Block, Opt. Lett. **19**, 930 (1994).

[7] A. Ashkin and J. M. Dziedzic, Science **235**, 1517 (1987).

[8] A. Ashkin, Proc. Natl. Acad. Sci. **94**, 4853 (1997).

[9] M. Mahamdeh and E. Schäffer, Opt. Express **17**, 17190 (2009).

[10] R. Grimm, M. Weidemuller, and Y. B. Ovchinnikov, Adv. At. Mol. Opt. Phys. **42**, 95 (2000).

[11] S. Tojo, T. Hayashi, T. Tanabe, T. Hirano, Y. Kawaguchi, H. Saito, and M. Ueda, Phys. Rev. A **80**, 042704 (2009).

[12] D. M. Stamper-Kurn and M. Ueda, Rev. Mod. Phys. **85**, 1191 (2013).

[13] A. L. Gaunt, T. F. Schmidutz, I. Gotlibovych, R. P. Smith, and Z. Hadzibabic, Phys. Rev. Lett. **110**, 200406 (2013).

[14] J. Leónard, M. Lee, A. Morales, T. M. Karg, T. Esslinger, and T. Donner, New J. Phys. **16**, 093028 (2014).

[15] A. Szczepkowicz, L. Krzemién, A. Wojciechowski, K. Brzozowski, M. Krüger, M. Zawada, M. Witkowski, J. Zachorowski, and W. Gawlik, Phys. Rev. A **79**, 013408 (2009).

[16] T. Bienaimé, S. Bux, E. Lucioni, Ph. W. Courteille, N. Piovella, and R. Kaiser, Phys. Rev. Lett. **104**, 183602 (2010).

[17] R. R. Agayan, F. Gitles, R. Kopelman, and C. F. Schmidt, Appl. Opt. **41**, 2318 (2002).

[18] H. Metcalf and P. van der Straten, *Laser Cooling and Trapping* (Springer Verlag, New York, USA, 1999).

[19] H. Chiba and H. Saito, Phys. Rev. A **78**, 043602 (2008).

[20] L. Mandel and E. Wolf, *Optical Coherence and Quantum Optics* (Cambridge University Press, New York, 1995).

[21] P. D. Lett, W. D. Phillips, S. L. Rolston, C. E. Tanner, R. N. Watts, and C. I. Westbrook, J. Opt. Soc. Am. B **6**, 2084 (1989).

[22] R. Dumke, M. Johanning, E. Gomez, J. Weinstein, K. Jones, and P. Lett, New J. Phys. **8**, 64 (2006).

[23] K. Shibata, S. Yonekawa, and S. Tojo, Phys. Rev. A **96**, 013402 (2017).

[24] A. Hemmerich, M. Weidemüller, T. Esslinger, C. Zimmermann, and T. Hänsch, Phys. Rev. Lett. **75**, 37 (1995).

[25] D. Boiron, A. Michaud, P. Lemonde, Y. Castin, C. Salomon, S. Weyers, K. Szymaniec, L. Cognet, and A. Clairon, Phys. Rev. A **53**, R3734 (1996).

[26] V. V. Klimov, D. Bloch, M. Ducloy, and J. R. Rios Leite, Phys. Rev. A **85**, 053834 (2012).

[27] P. Shumyatsky, G. Milione, and R. R. Alfano, Opt. Commun. **321**, 116 (2014).

[28] M. Greiner, O. Mandel, T. Esslinger, T. W. Hänsch, and I. Bloch, Nature **415**, 39 (2002).